Journal of Geochemical Exploration 178 (2017) 55–66

Contents lists available at ScienceDirect

Journal of Geochemical Exploration

journal homepage: www.elsevier.com/locate/gexplo

Application of spatially weighted technology for mapping intermediate and felsic igneous rocks in Fujian Province, China

Daojun Zhang [a,*], Qiuming Cheng [b,**], Frits Agterberg [c]

[a] College of Economics and Management, Northwest A&F University, Yangling 712100, China
[b] State Key Laboratory of Geological Processes and Mineral Resources, China University of Geosciences, Beijing 100083, Wuhan 430043, China
[c] Geological Survey of Canada, 601 Booth Street, Ottawa, ON K1A0E8, Canada

ARTICLE INFO

Article history:
Received 19 February 2016
Revised 27 January 2017
Accepted 26 March 2017
Available online 29 March 2017

Keywords:
Weak information extraction
Spatial variability
Local singularity analysis
Spatially weighted logistic regression
Mineral resource assessment
Igneous rocks

ABSTRACT

Magmatic activity is of great significance to mineralization not only for heat and fluid it provides, but also for parts of material source it brings. Due to the cover of soil and vegetation and its spatial nonuniformity detected signals from the ground's surface may be weak and of spatial variability, and this brings serious challenges to mineral exploration in these areas. Two models based on spatially weighted technology, i.e., local singularity analysis (LSA) and spatially weighted logistic regression (SWLR) are applied in this study to deal with this challenge. Coverage cannot block the migration of geochemical elements, it is possible that the geochemical features of soil above concealed rocks can be different from surrounding environment, although this kind of differences are weak; coverage may also weaken the surface expression of geophysical fields. LSA is sensitive to weak changes in density or energy, which makes it effective to map the distribution of concealed igneous rock based on geochemical and geophysical properties. Data integration can produce better classification results than any single data analysis, but spatial variability of spatial variables caused by non-stationary coverage can greatly affect the results since sometimes it is hard to establish a global model. In this paper, SWLR is used to integrate all spatial layers extracted from both geochemical and geophysical data, and the iron polymetallic metallogenic belt in south-west of Fujian Province is used as s study case. It is found that LSA technique effectively extracts different sources of geologic anomalies; and the spatial distribution of intermediate and felsic igneous rocks delineated by SWLR shows higher accuracy compared with the result obtained via global logistic regression model.

1. Introduction

Different geological environments, temperatures, pressures, and magma cycles create different mechanisms of mineral formation and migration, and these in turn, can cause geochemical and geophysical differences between intrusive rocks and their surroundings. This makes it possible to distinguish different intrusions from their surroundings. However, due to the effects of soil and vegetation cover, geochemical signatures and geophysical features obtained at the surface of the Earth may be weak. Hence, it is difficult to extract this weak information effectively by using classical data processing methods based on frequency statistics. Cheng and his team have developed a new spatial statistical method based on fractal/multifractal theory, called local singularity analysis (LSA) (Cheng, 1997, 2001, 2004, 2006a, 2006b, 2006c), which can supplement classic geological statistical techniques. LSA is essentially a spatial neighborhood-window statistical method that considers the original value of each spatial location as well as the trends in variation of these values within a local window. This method can detect slight changes in spatial locations and quantify them for the purpose of extracting local singularity information, while avoiding interference from the surface media, to reveal deep geological features of the underground environment. For this reason, LSA has been used to map concealed rocks based on both geochemical data (Cheng, 2012; Zhao et al., 2012) and geophysical data (Wang et al., 2012).

Geochemical data and geophysical data were obtained to represent the chemical properties and the physical characteristics of rocks, respectively. These two different types of data were combined with one another using data integration methods, which can improve the accuracy and efficiency of intrusive rock mapping. Many different models for data integration have been applied in mineral prospectivity mapping, including logistic regression (Tukey, 1972; Agterberg, 1974, 1988; Chung and Agterberg, 1980; Wrigley and Dunn, 1986), weights-of-evidence (Bonham-Carter et al., 1988, 1989; Agterberg, 1989; Agterberg et al., 1990), fuzzy logic (An et al., 1991; Bonham-Carter, 1994) and neural networks (Singer and Kouda, 1996, 1997; Oh and Lee, 2010). Although

* Corresponding author.
** Correspondence to: Q. Cheng, State Key Laboratory of Geological Processes and Mineral Resources, China University of Geosciences, Beijing 100083, Wuhan 430043, China.
E-mail addresses: zdj@nwsuaf.edu.cn (D. Zhang), qiuming@yorku.ca (Q. Cheng).

http://dx.doi.org/10.1016/j.gexplo.2017.03.015
0375-6742/

these methods have been integrated into GIS software and can be used to deal with spatial data, the locations and neighborhoods of spatial objects are always ignored and the relationship between location attribute and other attributes are completely separated, thus there is no essential difference between these methods and classical statistics. In fact, the intensity and structure of correlations between the target variable and independent variables may be changed from place to place due to spatial heterogeneity and non-stationary. The development of geographically weighted regression (GWR) changes this condition (Brunsdon et al., 1996; Fotheringham et al., 1996, 1997, 2002). GWR is a spatially varying-coefficient model, in which regression model is performed within a local window at each location, and inverse distance weighted (IDW) model is applied to achieve weigh reduction from current location to the edges of local window. The grids near to the current location are given greater weight while those far from the current location given less weight or even 0. There are some applications of GWR in mineral prospectivity mapping, e.g., Zhao et al. (2013, 2014) used GWR to analyze the quantitative relationship and its changes between the iron resources and the ore-controlling factors in the east Tianshan Mountain, and provided an improved prediction map for iron deposits. But yet there are few reports about geographically weighted logistic regression method in mineral exploration, while the latter is more suitable since mineralization is a binary event. The first author developed a spatially weighted logistic regression (SWLR) model for mineral prospectivity mapping (Zhang, 2015), and in this study, this model was used for intermediate and felsic igneous rocks mapping. Local singularity analysis (LSA) technique was used to process geochemical and geophysical data in order to obtain individual factor maps for intermediate and felsic rocks, and then based on a map of known Mesozoic intermediate and felsic rocks, general logistic regression and SWLR were applied respectively to integrate these individual maps for delineating target areas that could indicate the location of concealed intermediate and felsic igneous rocks. Our study is an initial attempt of using spatially weighted local model to deal with geological exploration mapping problem, and hoping that it can provide a new idea for similar research in this field.

2. Methods

2.1. Local singularity analysis (LSA)

Fractal/multifractal models are representative tools of nonlinear science that have been used for extraction of metallogenic information ever since nonlinear science techniques were developed. Fractal theory was initially used to characterize self-similar properties of geometric objects at different scales when the parts amplified were like the whole to some degree (Mandelbrot, 1975; Cheng et al., 1994; Cheng, 2016). Later, fractal/multifractal modeling was used to describe natural events with singularities, such as earthquakes, clouds, mountain torrents, hurricanes, landslides and wildfires, when there was a fractal/multifractal (or power-law) relationship between the frequency and size of the objects under study (Schertzer and Lovejoy, 1987; Bak et al., 1992; Malamud et al., 1996; Turcotte, 1997; Veneziano, 2002; Malamud et al., 2004; Sornette, 2004). Additionally, Cheng (1994) brought spatial information to bear on the power-law relationship and developed the concentration-area (C-A) model, which was considered as the first attempt to use fractal method to separate geochemical anomalies from background (Li et al., 2003). Later, Cheng (1997, 1999, 2005) proposed local singularity analysis (LSA) technology which can be seen as an application of the C-A model within a local window for local anomaly information extraction.

The most important choice that needs to be made during LSA, is the selection of an appropriate window size for the calculation of the local singularity index. The optimum window size is usually defined experimentally. If the window size is too small, LSA captures detailed information may include random noise, whereas a window size that is too large results in relatively smooth maps with less resolution. The singularity index is obtained by the following power-law model (Cheng, 1997):

$$\rho(\varepsilon) = c\varepsilon^{\alpha-2} \tag{1}$$

where c is a constant, ε represents window size, ρ represents average local density within a local window of size ε, and α is the singularity

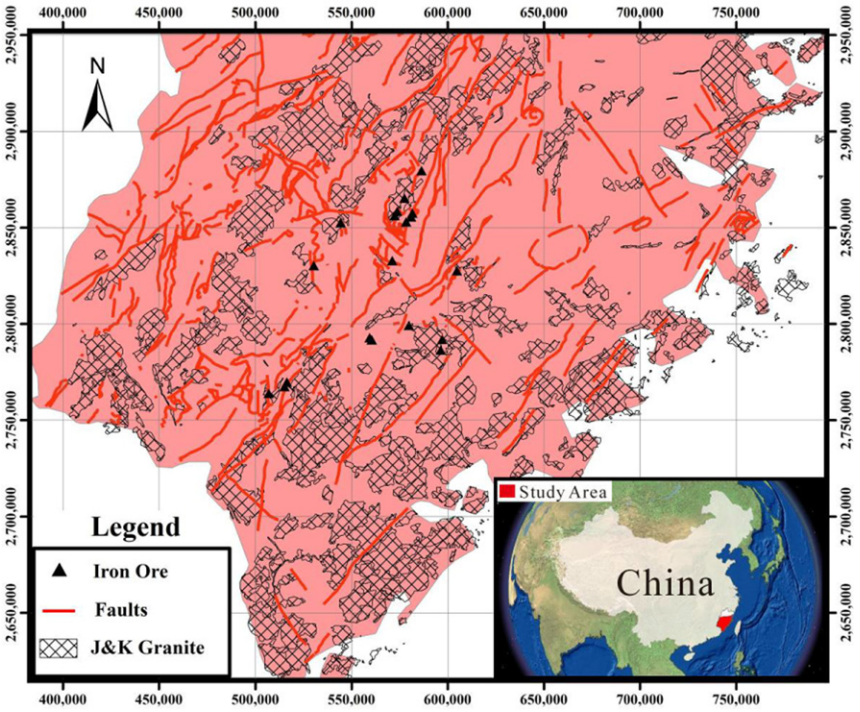

Fig. 1. The location of the study area, where J&K Granite represents the intermediate and felsic igneous rocks formed in Jurassic and Cretaceous of Mesozoic era.

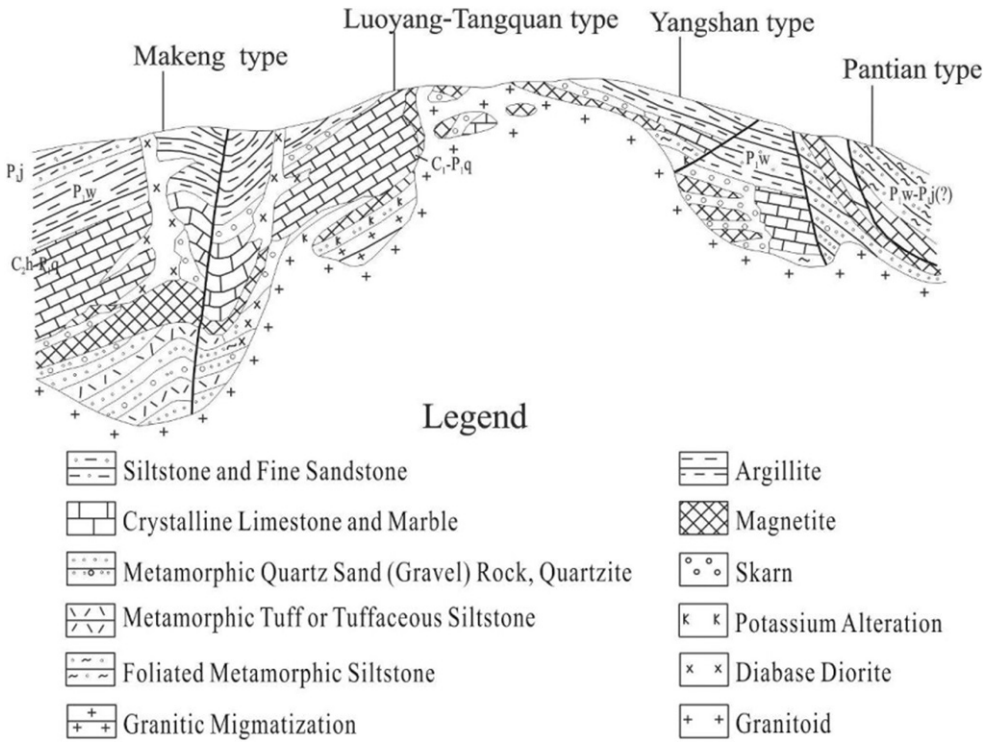

Fig. 2. The sketch of Makeng stratabound skarn type iron ore genesis model (Zhao et al., 1983).

index that can be estimated by least squares as the slope of a straight line fitted to the relationship between log ρ and log ε. The local singularity index α has the following properties: (1) when α is close to 2, the element concentration is relatively constant regardless of the window size; (2) when $\alpha < 2$, concentrations increase with the narrowing of window size, which indicates that the environment was enriched during the process of mineralization; and (3) when $\alpha > 2$, concentrations decrease with the narrowing of window size, which indicates depletion. Magmatic activity can also be viewed as a non-linear process. Therefore, as a product of magmatic activity, the spatial distribution of intermediate and felsic igneous rocks can also be considered as a singularity. It is clear that the sliding window is used in LSA, and sliding

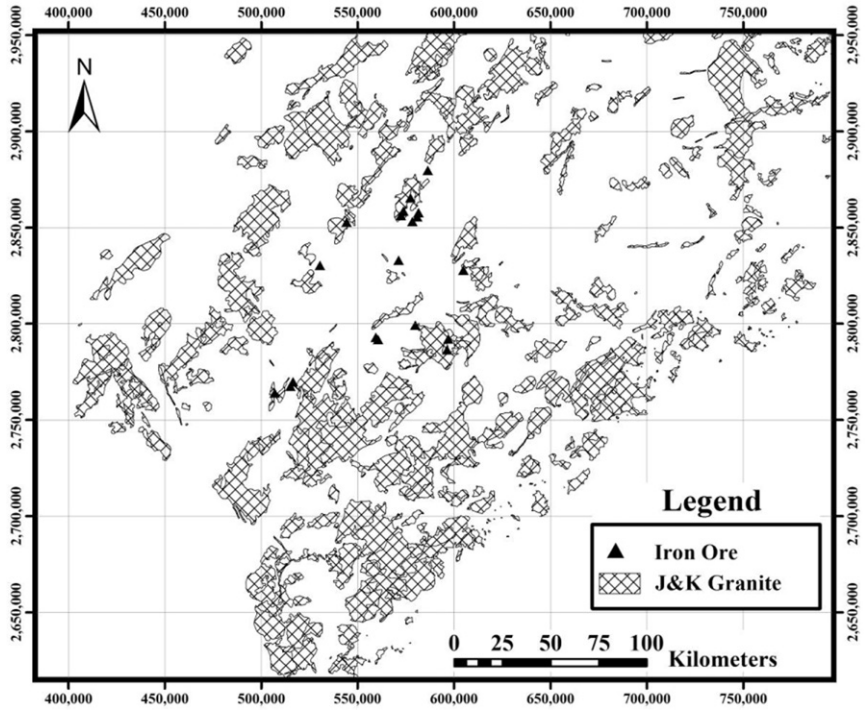

Fig. 3. Distribution of Jurassic-Cretaceous intermediate and felsic igneous rocks, and iron deposits.

window can be seen as a special case of spatial weighting, i.e. samples within the sliding window are weighted as 1 and others are weighted as 0. Therefore, LSA is also a spatially weighted model.

2.2. Spatially weighted logistic regression (SWLR)

Linear regression is commonly used for exploring the relationship between a response variable and one or more explanatory variables. In some research fields, such as in mineral prediction, the response variable is binary or dichotomous, linear regression will not be applicable in this case, then logistic regression model can show its advantage.

2.2.1. General logistic regression (GLR)

Suppose that $X_1, X_2, \ldots, X_p$ is a sample of p explanatory variables $x_1, x_2, \ldots, x_p$, and Y is a binary variable that can only assume the values of 1 and 0, then the following function can be used to estimate the probability that Y takes the value of 1:

$$P(Y=1|X_1,X_2,\ldots,X_p)=\pi(X)=\frac{e^{\beta_0+\beta_1x_1+\ldots+\beta_px_p}}{1+e^{\beta_0+\beta_1x_1+\ldots+\beta_px_p}} \quad (2)$$

and the probability that Y takes the value of 0 can be expressed as:

$$P(Y=0|X_1,X_2,\ldots,X_p)=1-\pi(X)=\frac{1}{1+e^{\beta_0+\beta_1x_1+\ldots+\beta_px_p}} \quad (3)$$

where π is the estimation of Y, β_0 is intercept, and $\beta_1, \beta_2, \ldots, \beta_p$ are regression coefficients. A Logit transformation about $P(Y=1|X_1,X_2,\ldots,X_p)$ can be performed based on Eqs. (2) and (3), then a linear function is obtained:

$$g(X)=\mathrm{Logit}\pi(X)=\ln\frac{\pi(X)}{1-\pi(X)}=\beta_0+\beta_1x_1+\ldots+\beta_px_p \quad (4)$$

If there are n samples, we can obtain n linear equations with $p+1$ unknowns based on Eq. (4). Further suppose that the observed values for Y are $y_1, y_2, \ldots, y_n$, and these observations are independent of each other, likelihood function can be established:

$$L(\beta)=\prod_{i=1}^{n}\pi(x_i)^{y_i}(1-\pi(x_i))^{1-y_i} \quad (5)$$

where $\pi(x_i)=\frac{e^{\beta_0+\beta_1x_{i1}+\ldots+\beta_px_{ip}}}{1+e^{\beta_0+\beta_1x_{i1}+\ldots+\beta_px_{ip}}}$. The best estimation can be obtained if and

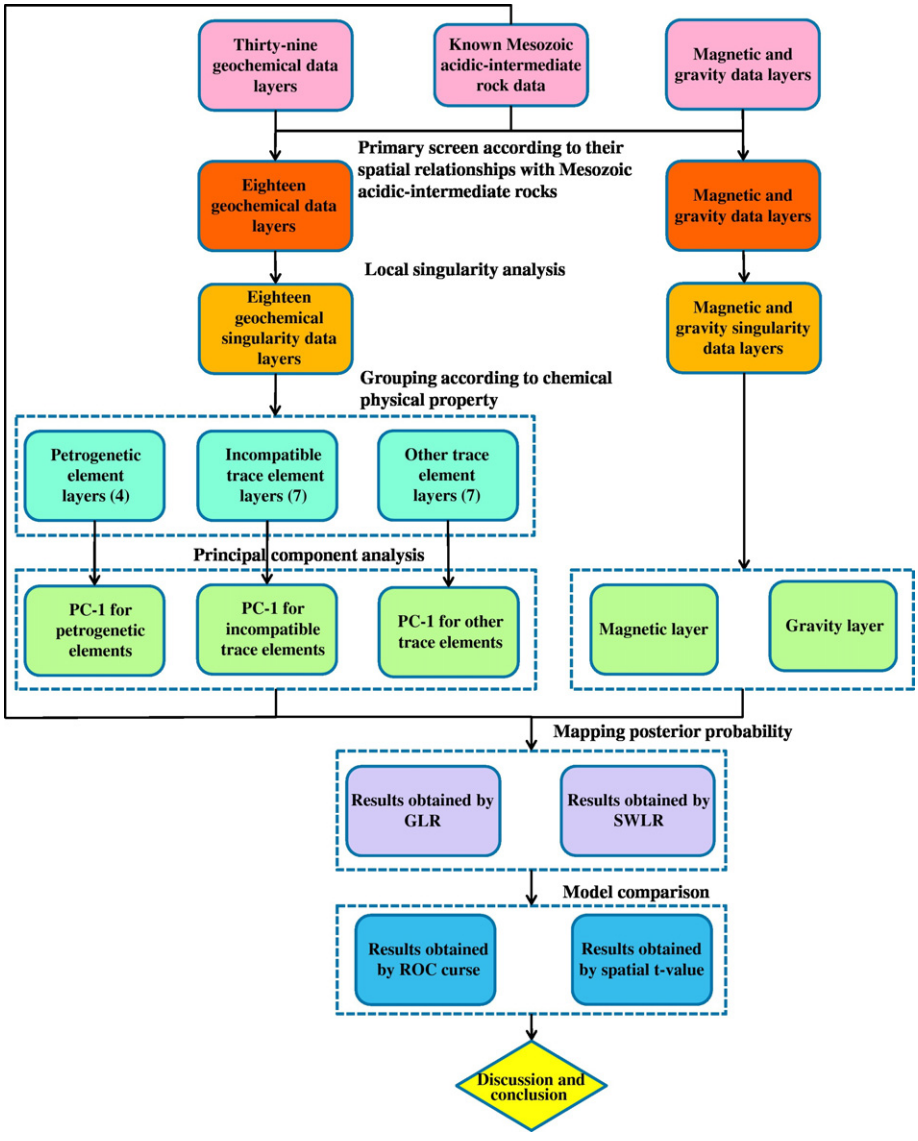

Fig. 4. Data processing flow and the structure for case study.

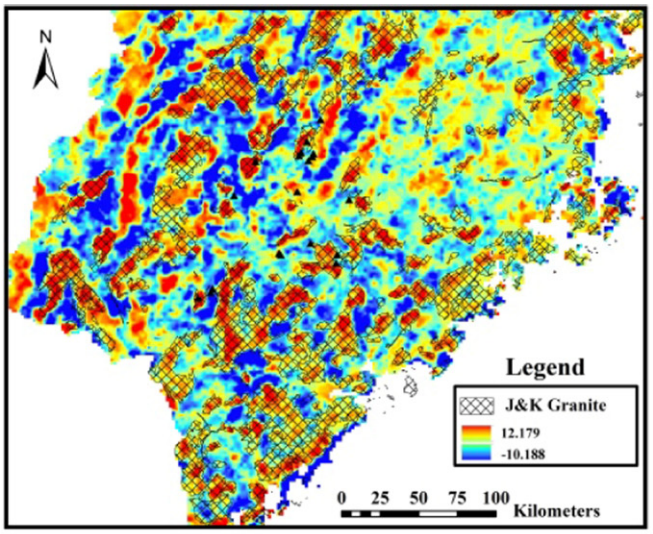

(a)

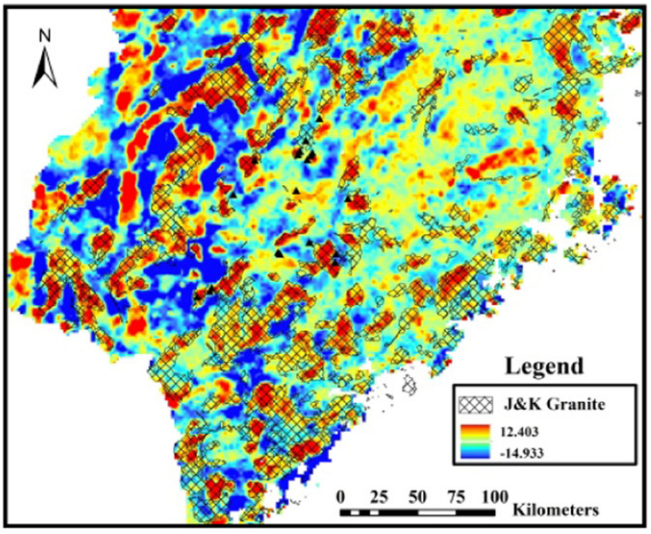

(b)

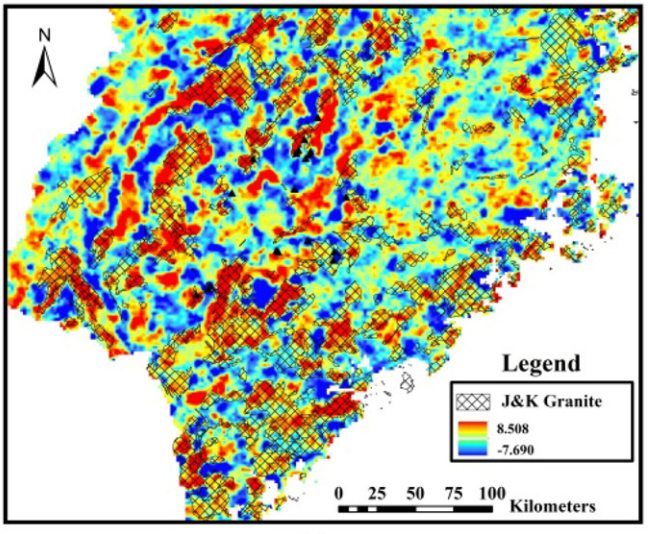

(c)

Fig. 5. Independent-variable for mapping intermediate and felsic igneous rocks, i.e., (a) PC-1 for local singularity index maps of selected petrogenetic elements which included Al_2O_3, K_2O, NaO and SiO_2, (b) PC-1 for local singularity index maps of selected incompatible trace elements which included Be, La, Nb, Th, U, Y and Zr, (c) PC-1 for local singularity index maps of selected other trace elements which included As, B, Cr, Mo, Ni, Pb and Sb.

only if Eq. (5) takes the maximum. Then the problem is converted to solve $\beta_0, \beta_1, \ldots \beta_p$. Eq. (5) can be further transformed into a log-likelihood function:

$$\ln L(\beta) = \sum_{i=1}^{n} (y_i \pi(x_i) + (1-y_i)(1-\pi(x_i))) \tag{6}$$

Its solution can be obtained by taking the first partial derivative of β_i ($i = 0$ to p), then Eq. (7) is obtained in the form of matrix operations.

$$\mathbf{X^T}(\mathbf{Y}-\boldsymbol{\pi}) = 0 \tag{7}$$

Newton-iterative method can be used to solve the nonlinear equations:

$$\beta(t+1) = \beta(t) + \mathbf{H}^{-1}\mathbf{U} \tag{8}$$

where $\mathbf{U} = \mathbf{X^T}(\mathbf{Y} - \boldsymbol{\pi}(t))$, t represents the number of iterations, $\mathbf{H} = \mathbf{X^T V}(t)\mathbf{X}$, and $\mathbf{V}(t), \mathbf{X}, \mathbf{Y}, \boldsymbol{\pi}(t)$ and $\boldsymbol{\beta}(t)$ are obtained as following:

$$\mathbf{V}(t) = \begin{pmatrix} \pi_1(t)(1-\pi_1(t)) & & & \\ & \pi_2(t)(1-\pi_2(t)) & & \\ & & \ddots & \\ & & & \pi_n(t)(1-\pi_n(t)) \end{pmatrix},$$

$$\mathbf{X} = \begin{pmatrix} x_{10} & x_{11} & \cdots & x_{1p} \\ x_{20} & x_{21} & \cdots & x_{2p} \\ \vdots & \vdots & \ddots & \vdots \\ x_{n0} & x_{n1} & \cdots & x_{np} \end{pmatrix}, \mathbf{Y} = \begin{pmatrix} y_1 \\ y_2 \\ \vdots \\ y_n \end{pmatrix}, \boldsymbol{\pi}(t) = \begin{pmatrix} \pi_1(t) \\ \pi_2(t) \\ \vdots \\ \pi_n(t) \end{pmatrix},$$

and $\boldsymbol{\beta}(t) = \begin{pmatrix} \beta_1(t) \\ \beta_2(t) \\ \vdots \\ \beta_n(t) \end{pmatrix}$.

The readers can see Hosmer et al. (2013) for more information about the derivation from Eqs. (2) to (8).

2.2.2. Spatially weighted logistic regression

Using π to represent the probability that y takes the value of 1, and $g(x) = \ln(\pi(x)/(1-\pi(x)))$ is the Logit form of $\pi(x)$, then spatially weighted logistic regression can be expressed as:

$$g_i(x,u) = logit(\pi_i(x,u)) = \beta_{0i}(x,u) + \beta_{1i}(x,u)x_{1i} + \beta_{2i}(x,u)x_{2i} + \cdots + \beta_{pi}(x,u)x_{pi} \tag{9}$$

where $\beta_{0i}(u), \beta_{1i}(u), \cdots, \beta_{pi}(u)$ mean that these parameters are obtaied at the location of u. The predicted probability for current location can be obtained in condition that the values of all independent variables at current location are known and all parameters are also calculated based on the samples within current local window. The parameters are estimated according to Eq. (10).

$$\hat{\beta}(u)_{t+1} = \hat{\beta}(u)_t + \left(\mathrm{X^T W}(u)\mathrm{V}(t)\mathrm{X}\right)^{-1}\mathrm{X^T W}(u)(\mathrm{Y}-\pi(t)) \tag{10}$$

where t represents the number of iterations; X is a matrix constituted by all independent variable values, and all elements in the first column are 1; $W(u)$ is a diagonal matrix, and the diagonal elements are geographical weights which can be calculated according to distance while other elements are all 0; $V(t)$ is also a diagonal matrix, and the diagonal element can be expressed as $\pi_i(t)(1-\pi_i(t))$; Y is a column vector representing the values dependent variable takes.

Besides geographic factor, the degree in studying can also affect the representative of the sample, e.g., differences in exploration level. In addition, we should also consider the sample size, especially when raster data is used. In order to avoid complex computation, Agterberg (1992) developed weighted logistic regression, in which all grids with the same values are merged into one class, and "unique condition" is used

to discribe the grids which have the same values in each layer (or variable). Unique condition area instead of grid is used to represent a sample, which greatly decreases the size of the matrix in estimating maximum likelihood parameters.

Suppose that there are n grids in current local window, S_i is the i-th grid, $W_i(g)$ is the geographical weight of S_i, and $W_i(d)$ represents individual difference weight (sometimes there exits quality or research degree differences among samples, and $W_i(d)$ takes the value of 1 if there is no this kind of differences), where i takes the value from 1 to n. Further suppose that there are N unique conditions after overlaying all layers, and C_j means the j-th unique condition unit, where $N \leqq n$, then we can obtain the final weight for each unique condition unit at current local window.

$$W_j(t) = \sum_{i=1}^{n} [W_i(g) * W_i(d) * df_i] \tag{11}$$

where $\begin{cases} df_i = 1, \text{if } S_i \in C_j \\ df_i = 0, \text{if } S_i \notin C_j \end{cases}$, j takes the value from 1to N; $W_j(t)$ represents the total weights (combining both $W_i(g)$ and $W_i(d)$) for each unique condition unit.

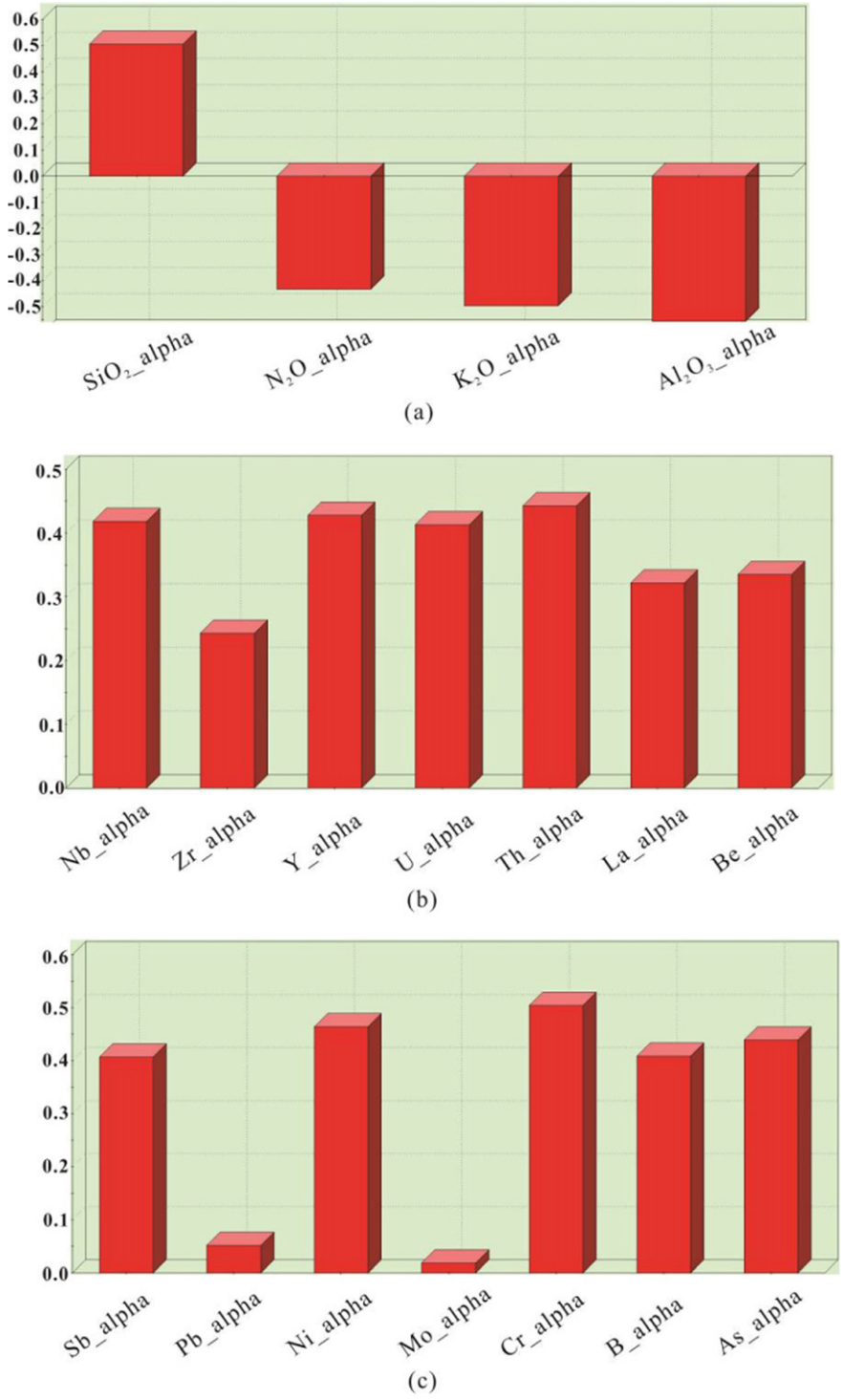

Fig. 6. The loadings on the first component obtained using Principle Component Analysis (PCA). From (a) to (c) are for petrogenetic elements, incompatible trace elements, and other trace elements respectively.

The equations from Eq. (9) to (11) are modified from the first author's doctoral thesis (Zhang, 2015) published in Chinese.

3. Study area and data

The Makeng iron polymetallic metallogenic belt lies in the southwest region of the Fujian Province, China (Fig. 1). Almost 98% of known iron deposits in Fujian are found in this region. In recent years, with increases in exploration and technological progress, a number of iron deposits have been discovered in this belt including the Makeng, Yangshan, Pantian, Luoyang, Zhongjia, and Panluo iron deposits. The belt is characterized by outcrops of Paleozoic strata and Mesozoic intermediate and felsic igneous rocks, which provides a favorable metallogenic environment for the formation of Fe, Cu, and Zn polymetallic deposits. According to the Fujian Institute of Geological Survey (2010), there is a great potential for undiscovered Makeng-type iron polymetallic deposits in this area. Although there are differences of opinions on the nature of the mineralization process and the genetic types of the deposits (Han and Ge, 1983a; Zhao et al., 1983; Jiang, 2007; Chen, 2010; Lin, 2011), it is widely accepted that this district experienced intense tectonic and magmatic activities that favored mineral enrichment. Some isotopic dating research supports the view that hydrothermal superimposition enriched mineralization in the Mesozoic strata (Han and Ge, 1983b; Mao et al., 2006; Wang et al., 2010; Lin, 2011). Fig. 2 depicts the metallogenic model given by Zhao et al. (1983), which shows that Makeng-type iron polymetallic deposits have a close relationship with skarnization. In this model, (1) the intrusion of Mesozoic intermediate and felsic magma provided sufficient heat for ore-forming fluids composed in part of iron; (2) the NNE/NW-treading faults provided a passageway, and (3) the presence of Carboniferous-Permian carbonate strata provided an excellent storage environment. Recent studies show that iron mineralization in this region often occurred in the contact zones between intrusions and late Paleozoic formations (Zuo et al., 2012; Zuo, 2016). As is shown in Fig. 3, most of the known deposits are situated around outcrops of intermediate and felsic igneous rocks. Hence, it is important to map the distribution of intermediate and felsic igneous rocks for predictions of Makeng-type iron mineralization (bolsters can also be found in Zuo et al., 2015; Zhang et al., 2015a, 2015b; Xiong and Zuo, 2016; Zhang et al., 2016). A portion of these rocks have been mapped in former geological surveys (see Fig. 3 for distribution of known intermediate and felsic igneous rocks). Fig. 3 illustrates the close relationship between the deposits and the intrusion of Mesozoic intermediate and felsic magma, but some intrusions were not mapped because they were concealed by soil and vegetation cover. Therefore, it is of great interest to find these concealed intermediate and felsic intrusions.

The datasets used in this study consisted of a geological map (1:250,000), stream sediment data (1:200,000), and magnetic and gravity data (1:200,000). Geochemical data (1:200,000) originated from China's National Geochemical Mapping Project and it was comprised of 39 major, minor, trace, and sub-trace elements. Following strategies are used for geochemical sampling: (i) high density sampling of 1 km^2, out of which four samples were composited into one sample representing 4 km^2, and (ii) low density sampling of one sample per 20–50 km^2 from areas of extremely difficult assess. Concentrations of Bi, Cd, Co, Cu, La, Mo, Nb, Pb, Th, U, and W elements were determined using inductively coupled plasma-mass spectrometry (ICP-MS). Concentrations of Al, Cr, Fe, K, P, Si, Ti, Y, and Zr were determined using X-ray fluorescence (XRF) spectrometry. Concentrations of Ba, Be, Ca, Li, Mg, Mn, Na, Ni, Sr, V, and Zn were determined using inductively coupled plasma-atomic emission spectrometry (ICP-AES). Concentrations of Ag, B, and Sn were determined using emission spectrometry (ES). Concentrations of As and Sb were determined using hydride generation-atomic fluorescence spectrometry (HG-AFS). Concentrations of Au, Hg, and F were determined through graphite furnace-atomic absorption spectrometry (GF-AAS), cold vapor-atomic fluorescence spectrometry (CV-AFS), and ion selective electrode (ISE) techniques, respectively (Xie et al., 1997, 2008). Geophysical datasets including ground-based Bouguer gravity data and airborne total magnetic intensity data with a 2-km spatial resolution were produced by the China Geological Survey (CGS). Mesozoic intermediate and felsic igneous layer was extracted from the geological map, which was also obtained from CGS (Zuo et al., 2015). All these data were transformed into grid data using ArcGIS 10.2 with the projection of the world's 50th zone (North), Universal Transverse Mercator coordinate system, the Datum of the World Geodetic System-1984 (WGS84), and a cell size of 2 km × 2 km.

4. Data processing and results

The data processing flow for this research is provided in Fig. 4, and more detailed explanation can be found in subsequent sections.

4.1. Variable selection and evidential layer preparation

General practice in rock mapping is to use only the rock-forming elements, while ignoring some of the trace elements and radioactive elements. However, some research on typical metallogenetic granitic

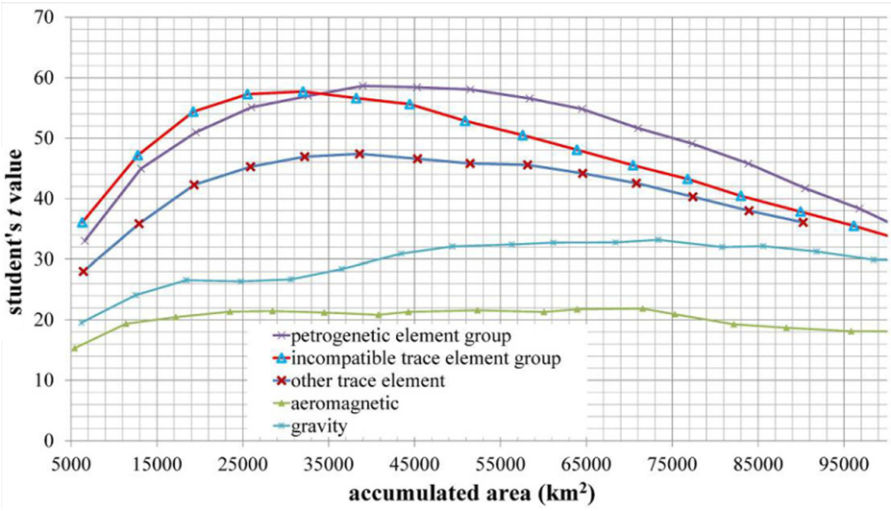

Fig. 7. Student's *t* values calculated for the spatial correlation between the known intermediate and felsic igneous rock layer and the five independent layers at different threshold levers.

bodies in the Fujian Province shows that the intermediate and felsic igneous rocks have certain geochemical features derived from primary elements, trace elements, and rare earth elements (Zhao, 2007; Qiu et al., 2012). We used data on 18 different elements and minerals (Al_2O_3, As, B, Be, Cr, K_2O, La, Mo, NaO, Nb, Ni, Pb, Sb, SiO_2, Th, U, Y, and Zr), which have been shown to have close spatial relationships with Mesozoic intermediate and felsic igneous rocks, along with magnetic and gravity data in our analyses. Next, following these steps to complete the data preparation.

(1) In order to initially weak the effect of spatial trend caused by field surface condition, LSA modeling was carried out with the local window size of 22 km to the 20 grid layers mentioned above with GeoDAS (GeoData Analysis System for Mineral Exploration and Environmental Assessment) software (Cheng, 2006b, 2012). One can also use a batch processing software module which is developed by the first author to improve efficiency and prediction accuracy (Zhang et al., 2016).
(2) Eighteen geochemical layers were further divided into 3 groups according to their chemical properties, i.e., petrogenetic element group (PE group) which included Al_2O_3, K_2O, NaO and SiO_2, incompatible trace elements (ICTE group) which included Be, La, Nb, Th, U, Y and Zr, and other trace elements (OTE group) which included As, B, Cr, Mo, Ni, Pb and Sb.
(3) Principal component analysis (PCA) was performed to reduce variate quantity, and the first principal components (PC-1s) for PE group, ICTE group and OTE group were obtained respectively, it is clear in Fig. 5 that all of the three layers are strongly highly relevant to the known Mesozoic intermediate and felsic igneous rocks. The plots of factor loadings for all of the three PC-1s are given in Fig. 6(a), (b) and (c) respectively, and it can be seen that almost all elements have high factor loading in the first principal component. That means the PC-1s can well represent the contribution of original elements. Besides, PC-1s occupied 61.5%, 54.3% and 37.3% of the total variance contributions for PE group, ICTE group and OTE group respectively.
(4) Three PC-1 layers (Fig. 5(a) to (c)) together with magnetic and gravity data layers were divided into 20-class layers using the quantile grouping method, and this is because discretization can improve the stability of sampled-data. These 5 independent variable layers would be used for data integration in following steps.

Table 1
Grid counts for each unique condition after overlaying all the independent-variable layers and the target variable layer. PE, ICTE, OTE and J&K Granite in the table headers are the abbreviations for petrogenetic element group which included Al_2O_3, K_2O, NaO and SiO_2, incompatible trace element group which included Be, La, Nb, Th, U, Y and Zr, other trace element group which included As, B, Cr, Mo, Ni, Pb and Sb, and the intermediate and felsic igneous rocks formed in Jurassic and Cretaceous of Mesozoic era respectively.

PE	ICTE	OTE	Aeromagnetic	Gravity	J&K granite	Grid numbers
1	1	1	1	1	1	1042
1	1	1	1	1	0	529
1	1	1	1	0	1	211
1	1	1	1	0	0	123
1	1	1	0	1	1	553
1	1	1	0	1	0	311
1	1	1	0	0	1	73
1	1	1	0	0	0	96
1	1	0	1	1	1	552
1	1	0	1	1	0	506
1	1	0	1	0	1	187
1	1	0	1	0	0	225
1	1	0	0	1	1	247
1	1	0	0	1	0	295
1	1	0	0	0	1	29
1	1	0	0	0	0	151
1	0	1	1	1	1	313
1	0	1	1	1	0	306
1	0	1	1	0	1	148
1	0	1	1	0	0	136
1	0	1	0	1	1	187
1	0	1	0	1	0	203
1	0	1	0	0	1	59
1	0	1	0	0	0	92
1	0	0	1	1	1	217
1	0	0	1	1	0	588
1	0	0	1	0	1	173
1	0	0	1	0	0	497
1	0	0	0	1	1	109
1	0	0	0	1	0	418
1	0	0	0	0	1	67
1	0	0	0	0	0	315
0	1	1	1	1	1	204
0	1	1	1	1	0	238
0	1	1	1	0	1	42
0	1	1	1	0	0	83
0	1	1	0	1	1	94
0	1	1	0	1	0	196
0	1	1	0	0	1	10
0	1	1	0	0	0	69
0	1	0	1	1	1	218
0	1	0	1	1	0	444
0	1	0	1	0	1	64
0	1	0	1	0	0	217
0	1	0	0	1	1	116
0	1	0	0	1	0	266
0	1	0	0	0	1	23
0	1	0	0	0	0	155
0	0	1	1	1	1	364
0	0	1	1	1	0	1001
0	0	1	1	0	1	159
0	0	1	1	0	0	655
0	0	1	0	1	1	216
0	0	1	0	1	0	852
0	0	1	0	0	1	59
0	0	1	0	0	0	520
0	0	0	1	1	1	576
0	0	0	1	1	0	3803
0	0	0	1	0	1	335
0	0	0	1	0	0	3729
0	0	0	0	1	1	335
0	0	0	0	1	0	2958
0	0	0	0	0	1	141
0	0	0	0	0	0	3005

4.2. Data integration

Based on the 5 independent-variable layers obtained above, GLR and SWLR modeling were performed respectively.

4.2.1. General logistic regression modeling

In traditional way, all independent variable layers are binary so that "1" means favorable and "0" means adverse for the target events. There are many methods which can be used for binaryzation, and spatial *t*-value is preferred in weights-of-evidence method (Agterberg, 1989;

Table 2
Estimates of regression coefficients.[a]

Variables	Beta	S.E.	Wald	Significance	Exponent (beta)
Petrogenetic element group	1.065	0.034	1004.401	0.000[b]	2.900
Incompatible trace element group	0.879	0.035	642.775	0.000[b]	2.408
Other trace element	0.814	0.031	671.473	0.000[b]	2.256
Aeromagnetic	0.397	0.032	156.764	0.000[b]	1.487
Gravity	0.491	0.033	216.374	0.000[b]	1.635
Constant	−2.735	0.038	5203.326	0.000[b]	0.065

[a] Analysis results extracted from IBM SPSS 20.0 software (with a slight change): there are five independent variables together with the constant in the first column; the second column represents regression coefficient while the third column represents their standard errors.
[b] In the sixth column means we can reject the H0 that the regression coefficient is equal to 0 when significance level is below 0.01, i.e., it is 99% sure that these regression coefficients are significantly different from 0.

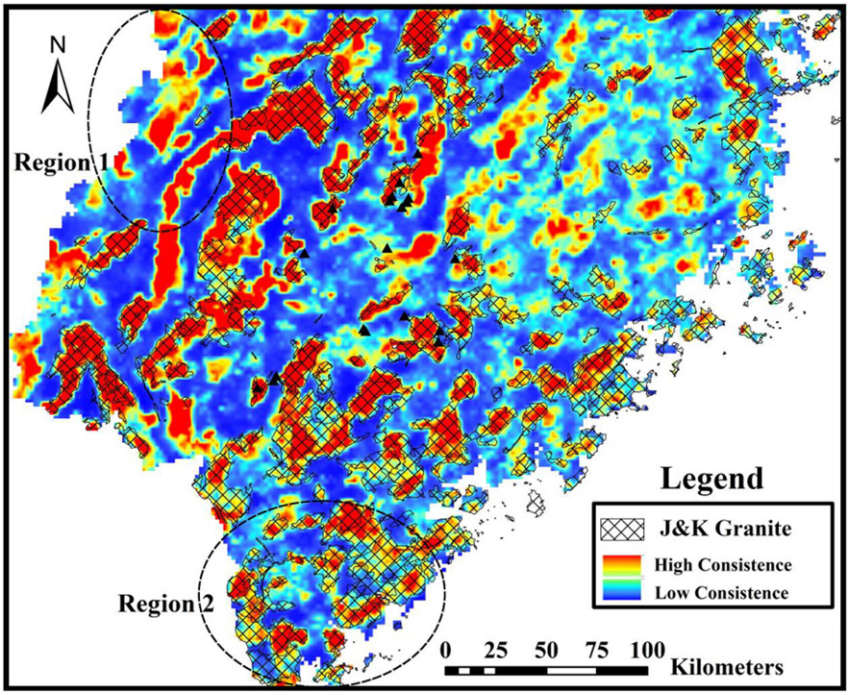

Fig. 8. Estimated probability map for intermediate and felsic igneous rocks obtained by general logistic regression.

Bonham-Carter et al., 1989). Here we also used spatial *t*-value to obtain a threshold for each independent variable layer. A bigger spatial *t*-value means a stronger spatial correlation between the independent variable layer and the target layer. As mentioned above, each independent variable layer has 20 status values with 19 binaryzation scenarios. According to spatial *t* statistics model, the best binaryzation scenario should have the highest spatial *t*-value. Based on this criterion, the threshold values were determined for the five independent-variable layers respectively (Fig. 7), and then they were transformed into binary grid layers. In ArcGIS 10.2, spatial overlay analysis was performed for the 5 layers together with the target layer which had already been transformed into a binary layer, and a new shapefile with a feather type of point is obtained. From the property sheet of the new established shapefile we can obtained $2^6 = 64$ unique condition records ideally according the values of the 6 original binary layers, and each of these records has a weight which is determined by the sample size of each unique condition (Table 1). Then GLR with weighting data is performed in SPSS 20.0, and the coefficient parameters were given in Table 2. It can be concluded from Table 2 that all

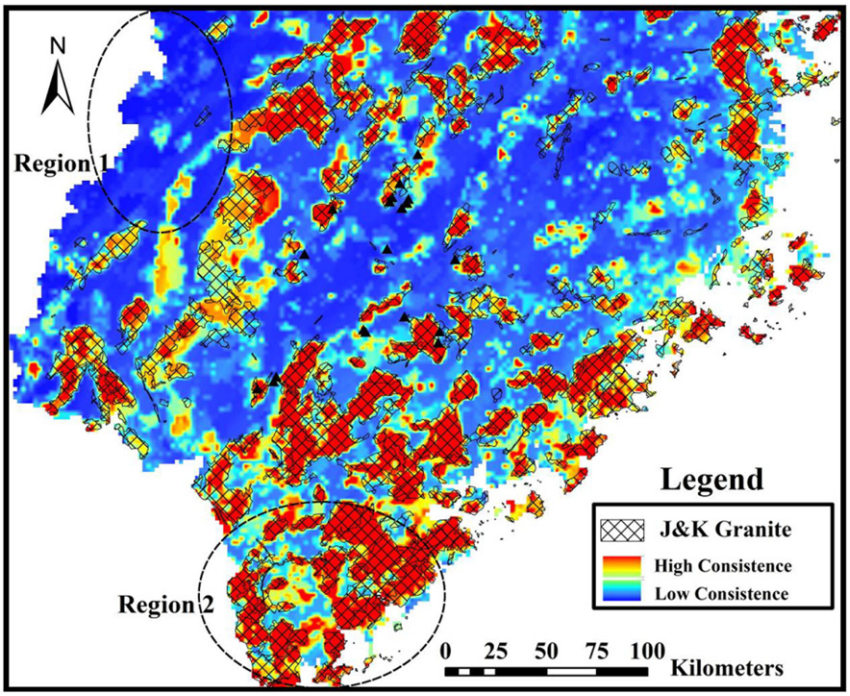

Fig. 9. Estimated probability map for intermediate and felsic igneous rocks obtained by spatially weighted logistic regression.

independent variables are correlated significantly with the target variable when significance level is 0.01 (Hosmer et al., 2013), and that means we have strong evidence that the coefficient parameters are not equal to 0. The probability map for Mesozoic intermediate and felsic igneous rocks was obtained in Fig. 8 using GLR model. As can been seen from Fig. 8, it is obvious that the probability map can fit the outcropped Mesozoic intermediate and felsic igneous rocks more or less except in some locations. For instance, it is most likely that there exists over-prediction in Region 1, while less-prediction may exist in Region 2. In order to deal with this problem, SWLR model will be applied in next section.

4.2.2. Spatially weighted logistic regression modeling

GLR belongs to global models, i.e., all grids in the study area are treated as the same importance, and the prediction in each location applies the same parameters obtained on the basis of the global model. Differences do exist among spatial samples according Tobler's First Law of Geography (Tobler, 1970), i.e., closer objects have stronger correlation than others, thus it is not suitable to treat all samples equally; in other words, a unified model cannot well deal with the variability of spatial variables since the predicted results may be biased. The process for SWLR is as follows.

(1) Determining the local window parameters

SWLR is a spatially varying-coefficient model, in which regression model is established within a local window to perform prediction with local optimal parameters at each location. Local window parameters for SWLR can be determined based on geological statistics theory (Zhang, 2015). This ideal is also adopted in this research. Here elliptic local window was used to describe spatial anisotropy changes with the application of ArcGIS Geostatistical Analyst provided in ArcGIS 10.2. According to the variogram function model, the length of semi-major axis was 94 km, the length ratio of major and minor axis was 0.3, and the orientation of the ellipse's major axis was 30° which was concordant with that of regional tectonics. In addition, Wald test is applied here to verify the significance of the logistic regression equation; if the null hypothesis could not be excluded on a 5% significance level, the length of semi-major axis would be increased iteratively. The largest semi-major axis was set as 188 km, which was sufficient to ensure there were enough known samples within the current local window. Exponential decay was applied to each grid according to its distance from the current location within the local window.

(2) Mapping with SWLR modeling

SWLR software tool developed by Zhang (2015) was used in this research. Because there are no quality or research degree differences in the study area, only spatial weights determined in last step are used in Eq. (11) in this research. The predicted probability map for intermediate and felsic igneous rocks is given in Fig. 9. It can be seen from Fig. 9 that the high value grids can not only fit the outcropped Mesozoic intermediate and felsic igneous rocks well as a whole, the locations which are not well predicted in Fig. 8, e.g. Regions 1 and 2, are also well predicted here. Some quantitative comparison methods will be applied in following section to evaluate the predict results obtained by both logistical regression and SWLR.

5. Model comparison and discussion

In this section, spatial *t*-value model is applied respectively to compare GLR and SWLR based on their abilities in predicting intermediate and felsic igneous rocks.

A threshold point is needed to delineate a target area, and there are many different methods that can be used for deriving this such as the C-A model, the standard deviation method (e.g., locations with values >3 times the standard deviation are delineated as the target area), and student's *t*-value, which is an important parameter that can measure the significance of spatial correlations between evidential layers and the target layer in WofE. The estimated probability maps obtained by GLR and SWLR were divided into 20 classes by the quantile method, and then, the *t*-values were calculated using WofE modeling (Fig. 10). It is obvious that SWLR lead to a better performance since greater *t*-values were obtained in SWLR. Using the maximum value among the *t*-values as break points, distribution maps of intermediate and felsic igneous rocks could be obtained by GLR and SWLR respectively (Fig. 11). In Fig. 11 (a), 26.64% of the total study area was divided as intermediate and felsic igneous rocks, and 73.01% of the target area were correctly mapped by SWLR; with respect to GLR. 53.50% of the target area were correctly predicted when 23.17% of the study area was divided as intermediate and felsic igneous rocks. The overall accuracy for SWLR and GLR were 84.31% and 78.49% respectively. It is obvious that SWLR provided a

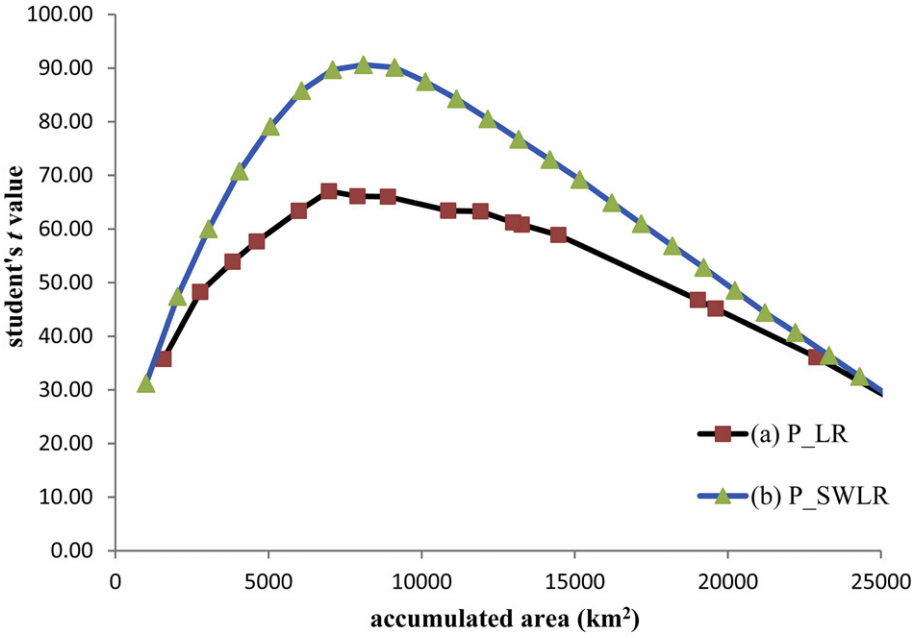

Fig. 10. Student's *t* values calculated for the spatial correlation between layers of the targeting layer and the predicting probability maps obtained by using (a) general logistic regression and (b) spatially weighted logistic regression respectively.

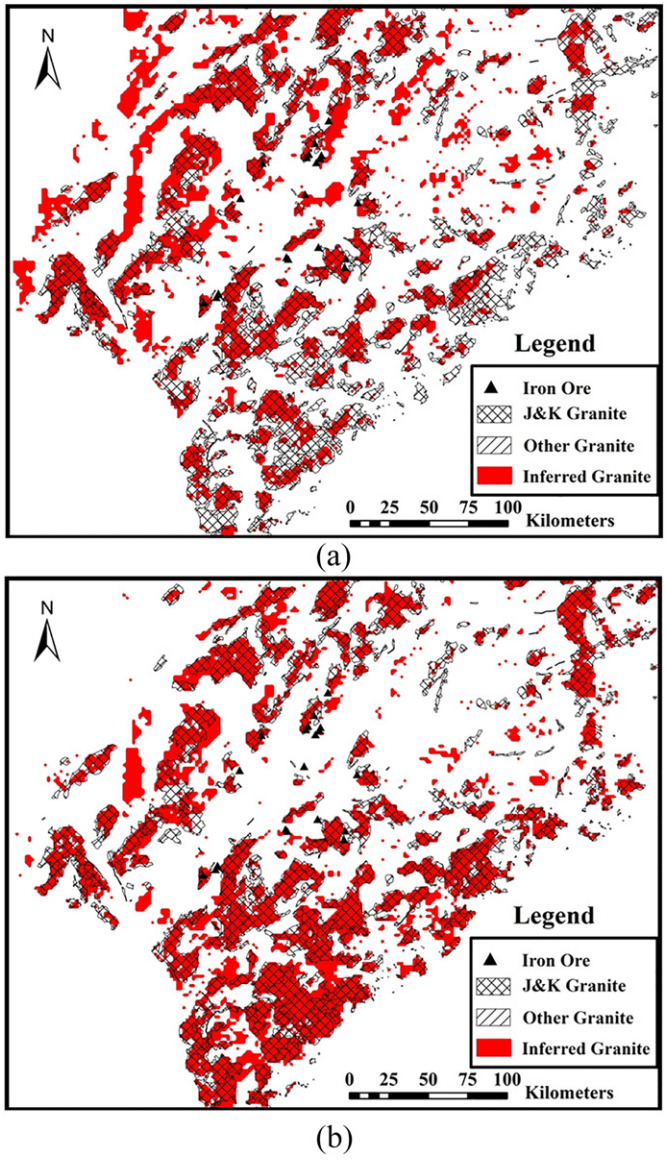

Fig. 11. Target delineation for the Mesozoic intermediate and felsic igneous rocks by using (a) general logistic regression and (b) spatially weighted logistic regression based on the maximum spatial *t* values in Fig. (9).

much better predicting result. The majority of the intermediate and felsic igneous rock outcrops were in the target areas obtained by SWLR and buried intermediate and felsic igneous rocks may exist in covered regions of the target area. It should be noted that only Mesozoic intermediate and felsic igneous rocks were used as training samples, but intermediate and felsic igneous rocks formed in other geologic ages were also well delineated in Fig. 11. What should be pointed out is that we used the variable layers obtained through LSA instead of initial layers for both SWLR and GLR modeling, thus it is fair to compare them in this study and the conclusion should be reliable.

6. Conclusions

In this study, spatially weighted technique was used for intermediate and felsic igneous rocks mapping. The LSA technique was used to process geochemical and geophysical data in order to obtain an individual factor map of intermediate and felsic rocks, and then based on a map of known Mesozoic intermediate and felsic rocks, GLR and SWLR was applied to integrate these individual maps for delineating target areas that could indicate the location of concealed mineral resources. The conclusions drawn from this study were as follows:

(1) Although rock-forming elements are more often used in rock type mapping, several trace elements, especially strong incompatible trace elements, were found to be useful for indicating the presence of intermediate and felsic igneous rocks in addition to the rock-forming elements.
(2) Due to the restrictions of uneven surface distribution and other environmental differences, spatial non-stationary does exist among spatial variables, and therefore it is necessary to adopt spatially weighted technique in spatial prediction. LSA and SWLR were applied in this research for information extraction and data integration respectively to overcome the adverse impact caused by spatial non-stationary, and they were proved to be effective in intermediate and felsic igneous rocks mapping.
(3) Known mineral deposits were mostly scattered along the boundary of intermediate and felsic igneous rocks, which confirms that these deposits belong to the contact-metasomatic type. Consequently, the buffer area for the boundary of intermediate and felsic igneous rocks will be one of the most important evidential layers for use in ore prospecting for this type of resource in the future. Although the direct purpose of this study was not ore prospecting, we found that magmatic activities had an important influence on mineralization. Since magmatic hydrothermal deposits are the main type of deposit on Earth, the results from this study will not only benefit further prospecting for Makeng-type iron in this region, but they may also provide a reference for searches for similar deposits around the world.

At last, due to the restrictions of uneven surface distribution and other environmental differences, spatial non-stationary does exist among spatial variables, and therefore it is necessary to adopt spatially weighted technique in spatial prediction. LSA and SWLR were applied in this research for information extraction and data integration respectively to overcome the adverse impact caused by spatial non-stationary, and they proved to be effective in intermediate and felsic igneous rocks. We compared SWLR to GLR in mapping intermediate and felsic igneous rocks. Nevertheless, neither of them could distinguish igneous rocks formed in different geological ages, which need the help of dating-technique to provide additional data.

Acknowledgments

This research has benefited from joint financial support of the Programs of Integrated Prediction of Mineral Resources in Covered Areas (No. 1212011085468), China Postdoctoral Science Foundation (No. 2016M592840), National Natural Science Foundation of China (No. 41602336), and the second batch of Fundamental Research from Northwest A&F University in 2015 (No. 2452015232).

References

Agterberg, F.P., 1974. Automatic contouring of geological maps to detect target areas for mineral exploration. J. Int. Assoc. Math. Geol. 6 (4), 373–395.
Agterberg, F.P., 1988. Application of recent developments of regression analysis in mineral resource evaluation. In: Chung, et al. (Eds.), Quantitative Analysis of Mineral and Energy Resources. D. Reidel Publishing Company, Dordrecht, pp. 1–28.
Agterberg, F.P., 1989. Computer programs for mineral exploration. Science 245, 76–81.
Agterberg, F.P., 1992. Combining indicator patterns in weights of evidence modeling for resource evaluation. Nonrenewal Res. 1 (1), 35–50.
Agterberg, F.P., Bonham-Carter, G.F., Wright, D.F., 1990. Statistical pattern integration for mineral exploration. In: Gaál, G., Merriam, D.F. (Eds.), Computer Applications in Resource Estimation Prediction and Assessment of Metals and Petroleum. Pergamon Press, New York, pp. 1–12.
An, P., Moon, W.M., Rencz, A., 1991. Application of fuzzy set theory for integration of geological, geophysical and remote sensing data. Can. J. Explor. Geophys. 27, 1–11.
Bak, P., Chen, K., Tang, C., 1992. A forest-fire model and some thoughts on turbulence. Phys. Lett. A14, 297–300.

Bonham-Carter, G.F., Agterberg, F.P., Wright, D.F., 1988. Integration of geological datasets for gold exploration in nova scotia. Photogramm. Eng. Remote Sens. 54 (11), 1585–1592.
Bonham-Carter, G.F., Agterberg, F.P., Wright, D.F., 1989. Weights of evidence modelling: a new approach to mapping mineral potential. In: Agterberg, F.P., Bonham-Carter, G.F. (Eds.), Statistical Applications in the Earth Sciences, pp. 171–183.
Bonham-Carter, G.F., 1994. Geographic Information Systems for Geoscientists: Modelling With GIS (No. 13). Elsevier.
Brunsdon, C., Fotheringham, A.S., Charlton, M.E., 1996. Geographically weighted regression: a method for exploring spatial nonstationarity. Geogr. Anal. 28 (4), 281–298.
Chen, Y., 2010. New understanding of ore control structure feature of Fujian Makeng iron mine. Met. Miner. 404, 96–99 (in Chinese with English abstract).
Cheng, Q., 1994. Multifractal Modeling and Spatial Analysis With GIS: Gold Potential Estimation in the Mitchell-Sulphurets Area, Northwestern British Columbia, Doctoral Dissertation. Univ. Ottawa, Ottawa.
Cheng, Q., 1997. Fractal/Multifractal Modeling and Spatial Analysis, Keynote Lecture in Proceedings of the International Mathematical Geology Association Conference. 1 pp. 57–72.
Cheng, Q., 1999. Multifractal interpolation. In: Lippard, S.J., Naess, A., Sinding-Larsen, R. (Eds.), Proceedings of the Fourth Annual Conference of the International Association for Mathematical Geology. Trondheim, Norway, pp. 245–250.
Cheng, Q., 2001. Multifractal and geostatistic methods for characterizing local structure and singularity properties of exploration geochemical anomalies. Earth Sci. J. China Univ. Geosci. 26, 161–166 (in Chinese with English abstract).
Cheng, Q., 2004. Quantifying the generalized self-similarity of spatial patterns for mineral resource assessment. Earth Sci. J. China Univ. Geosci. 29, 733–744 (in Chinese with English abstract).
Cheng, Q., 2005. A new model for incorporating spatial association and singularity in interpolation of exploratory data. Geostatistics Banff. 2004. Springer, pp. 1017–1025.
Cheng, Q., 2006a. GIS based fractal/multifractal anomaly analysis for modeling and prediction of mineralization and mineral deposits. In: Harris, J., Wright, D.F. (Eds.), GIS for Geosciences. Geological Association of Canada, pp. 285–296.
Cheng, Q., 2006b. Mapping singularities with stream sediment geochemical data for prediction of undiscovered mineral deposits in Gejiu, Yunnan Province, China. Ore Geol. Rev. 32, 314–324.
Cheng, Q., 2006c. Singularity-generalized self-similarity-fractal spectrum (3S) models. Earth Sci. J. China Univ. Geosci. 31, 337–348 (in Chinese with English abstract).
Cheng, Q., 2012. Singularity theory and methods for mapping geochemical anomalies caused by buried sources and for predicting undiscovered mineral deposits in covered areas. J. Geochem. Explor. 122, 55–70.
Cheng, Q., 2016. Fractal density and singularity analysis of heat flow over ocean ridges. Sci. Rep. http://dx.doi.org/10.1038/srep19167.
Cheng, Q., Agterberg, F.P., Ballatyne, S.B., 1994. The separation of geochemical anomalied from background by fractal methods. Explor. Geochem. 51, 109–130.
Chung, C.F., Agterberg, F.P., 1980. Regression models for estimating mineral resources from geological map data. Math. Geol. 12, 473–488.
Fujian Institute of Geological Survey, 2010. The Report of Iron Potential Evaluation. p. 148 (in Chinese).
Fotheringham, A.S., Brunsdon, C., Charlton, M.E., 1996. The geography of parameter space: an investigation of spatial non-stationarity. Int. J. Geogr. Inf. Syst. 10, 605–627.
Fotheringham, A.S., Brunsdon, C., Charlton, M.E., 2002. Geographically Weighted Regression: The Analysis of Spatially Varying Relationships. Wiley, Chichester.
Fotheringham, A.S., Charlton, M.E., Brunsdon, C., 1997. Two techniques for exploring nonstationarity in geographical data. Geogr. Syst. 4, 59–82.
Han, F., Ge, C., 1983a. Geological and geochemical features of submarine volcanic hydrothermal-sedimentary mineralization of Makeng iron deposit, Fujian Province. Bulletin of the Institute of Mineral Deposits. 2. Chinese Academy of Geological Sciences, pp. 60–87 (in Chinese with English abstract).
Han, F., Ge, C., 1983b. Makeng iron deposit: a submarine volcanic hydrothermal sedimentary deposit. Sci. China B 5, 438–455 (in Chinese with English abstract).
Hosmer, D.W., Lemeshow, S., Sturdivant, R.X., 2013. Applied Logistic Regression. third ed. Wiley, New York.
Jiang, Y., 2007. Discussion the genesis of the middle section of Makeng iron ore deposit. Express Information of Mining Industry. 7, pp. 69–77 (in Chinese with English abstract).
Li, C., Ma, T., Shi, J., 2003. Application of a fractal method relating concentrations and distances for separation of geochemical anomalies from background. J. Geochem. Explor. 77 (2), 167–175.
Lin, D., 2011. Research on Late Paleozoic-Triassic Tectonic Evolution and Metallogenetic Regularities of Iron-Polymetalic Deposits in the southwestern Fujian Province (Dissetation). (Doctoral Dissertation). China University of Geosciences, Beijing.
Malamud, B.D., Turcotte, D.L., Barton, C.C., 1996. The 1993 Mississippi river flood: a one hundred or a one thousand year event. Environ. Eng. Geosci. 2, 479–486.
Malamud, B.D., Turcotte, D.L., Guzzetti, F., Reichenbach, P., 2004. Landslide inventories and their statistical properties. Earth Surf. Process. Landf. 29, 687–711.
Mandelbrot, B.B., 1975. Stochastic models for the Earth's relief, the shape and the fractal dimension of the coastlines, and the number-area rule for islands. Proc. Natl. Acad. Sci. U. S. A. 72, 3825–3828.
Mao, J., Chen, R., Li, J., Ye, H., Zhao, X., 2006. Geochronology and geochemical characteristics of Late Mesozoic granotic rocks from southwestern Fujian and their tectonic evolution. Acta Petrol. Sin. 22, 1723–1734 (in Chinese with English abstract).
Oh, H.J., Lee, S., 2010. Application of artificial neural network for gold–silver deposits potential mapping: a case study of Korea. Nat. Resour. Res. 19, 103–124.
Qiu, J., Li, Z., Liu, L., Zhao, J., 2012. Petrogenesis of the Zhangpu composite granite pluton in Fujian Province: constraints from zircon U-Pb ages, elemental geochemistry and Nd-Hf isotopes. Acta Geol. Sin. 86, 561–576 (in Chinese with English abstract).
Schertzer, D., Lovejoy, S., 1987. Physical modeling and analysis of rain and clouds by anisot ropic scaling of multiplicative processes. J. Geophys. Res. 92, 9693–9714.
Singer, D.A., Kouda, R., 1996. Application of a feedforward neural network in the search for Kuruko deposits in the Hokuroku district, Japan. Math. Geol. 28, 1017–1023.
Singer, D.A., Kouda, R., 1997. Use of neural network to integrate geoscience information in the classification of mineral deposits and occurrences. In: Gubins, A.G. (Ed.), Proceedings of Exploration 97: 4th Decennial International Conference on Mineral Exploration, pp. 127–134.
Sornette, D., 2004. Critical Phenomena in Natural Sciences: Chaos, Fractals, Self Organization and Disorder. second ed. Springer, New York.
Tobler, W.R., 1970. A computer movie simulating urban growth in the Detroit region. Econ. Geogr. 46 (2), 234-24.
Tukey, J.W., 1972. Discussion of paper by FP Agterberg and SC Robinson. Bull. Int. Stat. Inst. 44 (1), 596.
Turcotte, D.L., 1997. Fractals and Chaos in Geology and Geophysics. second ed. Cambridge University Press, Cambridge.
Veneziano, D., 2002. Multif ractality of rainfall and scaling of intensity-duration-frequency curves. Water Resour. Res. 38, 1–12.
Wang, D., Chen, Z., Chen, Y., Tang, J., Li, J., Ying, L., Wang, C., Liu, S., Li, L., Qing, Y., Li, H., Qu, W., Wang, Y., Chen, W., Zhang, Y., 2010. New data of the rock-forming and ore-forming chronology for China's important mineral resources areas. Acta Geol. Sin. 84, 1030–1040 (in Chinese with English abstract).
Wang, W., Zhao, J., Cheng, Q., Liu, J., 2012. Tectonic-geochemical exploration modeling for characterizing geo-anomalies in southeastern Yunnan District, China. J. Geochem. Explor. 122, 71–80.
Wrigley, N., Dunn, R., 1986. Graphical diagnostics for logistic oil exploration models. Math. Geol. 18, 355–374.
Xie, X., Mu, X., Ren, T., 1997. Geochemical mapping in China. J. Geochem. Explor. 60, 99–113.
Xie, X., Wang, X., Zhang, Q., Zhou, G., Cheng, H., Liu, D., Cheng, Z., Xu, S., 2008. Multi-scale geochemical mapping in China. Geochem. Explor. Environ. Anal. 8, 333–341.
Xiong, Y., Zuo, R., 2016. A comparative study of two modes for mapping felsic intrusions using geoinformatics. Appl. Geochem. 75, 277–283.
Zhang, D., 2015. Spatially Weighted Technology for Logistic Regression and Its Application in Mineral Prospectivity Mapping (Dissertation). China University of Geosciences, Wuhan (in Chinese with English abstract).
Zhang, Z., Zuo, R., Cheng, Q., 2015a. Geological features and formation processes of the Makeng Fe deposit, China. Resour. Geol. 65, 266–284.
Zhang, Z., Zuo, R., Cheng, Q., 2015b. The mineralization age of the Makeng Fe deposit, South China: implications from U-Pb and Sm-Nd geochronology. Int. J. Earth Sci. 104, 663–682.
Zhang, D., Cheng, Q., Agterberg, F., Chen, Z., 2016. An improved solution of local window parameters setting for local singularity analysis based on excel VBA batch processing technology. Comput. Geosci. 88, 54–66.
Zhang, Z., Zuo, R., Xiong, Y., 2016. A comparative study of fuzzy weights of evidence and random forests for mapping mineral prospectivity for skarn-type Fe deposits in the southwestern Fujian metallogenic belt, China. Sci. Chi. Earth Sci. 59, 556–572.
Zhao, J., Wang, W., Cheng, Q., 2013. Investigation of spatially non-stationary influences of tectono-magmatic processes on Fe mineralization in eastern Tianshan, China with geographically weighted regression. J. Geochem. Explor. 134, 38–50.
Zhao, J., Wang, W., Cheng, Q., 2014. Application of geographically weighted regression to identify spatially non-stationary relationships between Fe mineralization and its controlling factors in eastern Tianshan, China. Ore Geol. Rev. 57, 628–638.
Zhao, J., Wang, W., Dong, L., Yang, W., Cheng, Q., 2012. Application of geochemical anomaly identification methods in mapping of intermediate and felsic igneous rocks in eastern Tianshan, China. J. Geochem. Explor. 122, 81–89.
Zhao, X., 2007. The Geochronology Petrography and Geochemical Characteristics of Mesozoic Granitoids From Shanghang Area in SW Fujian and Their Implications. Chinese Academy of Geological Sciences, Beijing (Master's Dissertation, in Chinese with English abstract).
Zhao, Y., Tan, H., Xu, Z., Yuan, R., Bi, C., Zhen, L., Li, D., Sun, J., 1983. The calcic-skarn iron ore deposit of Makeng type in southwestern Fujian. Bulletin of the Institute of Mineral Deposits. 1. Chinese Academy of Geological Sciences, pp. 1–141 (in Chinese).
Zuo, R., Xia, Q., Zhang, D., Cheng, Q., 2012. Geological process-based mineral resource quantitative prediction and assessment for making type iron polymetallic deposits in Fujian. Earth Sci. J. China Univ. Geosci. 37, 1183–1190 (in Chinese with English abstract).
Zuo, R., Zhang, Z., Zhang, D., Carranza, E.J.M., Wang, H., 2015. Evaluation of uncertainty in mineral prospectivity mapping due to missing evidence: A case study with skarn-type Fe deposits in southwestern Fujian Province, China. Ore Geol. Rev. 71, 502–515.